Structure and Dynamics of the Modular Halves of *Escherichia coli* Cyclic AMP Receptor Protein†

Jianquan Li, Xiaodong Cheng,‡ and J. Ching Lee*

Department of Human Biological Chemistry and Genetics, The University of Texas Medical Branch at Galveston, Galveston, Texas 77555-1055

Received July 1, 2002; Revised Manuscript Received October 1, 2002

ABSTRACT: *E. coli* cyclic AMP receptor protein, CRP, is a modular protein that consists of a covalent linkage of two common structural domains. To probe the mechanism for intramolecular communications and to define the unique properties acquired by covalent linkage, the structural, and functional properties of the cAMP- and DNA-binding domains of CRP were studied separately as two independent polypeptides. The N-terminal cAMP-binding domain (α-CRP), including S-CRP and CH-CRP, which were generated by digestion of CRP by subtilisin and chymotrypsin, respectively, are mainly populated by β-sheets. The C-terminal DNA-binding domain, designated as β-CRP, consists of mostly α-helices. The residues of S-CRP and CH-CRP are from 1 to 116 and 1 to 136 of intact wild-type CRP, and those of β-CRP are from 108 to 209. The secondary structures of α-CRP and β-CRP were monitored by FT-IR, and they are similar to those of the corresponding parts in intact wild-type CRP. Results from hydrogen−deuterium exchange experiments indicated that β-CRP is more dynamic than α-CRP. In an earlier study, it was shown that α-CRP retains the function of binding cAMP [Heyduk, E., et al. (1992) *Biochemistry 31*, 3682−3688]. β-CRP was able to bind to DNA, although only weakly, and was not sequence specific. Thus, a covalent linkage between the two domains is essential for the realization of the intramolecular signal transmission between the domains triggered by ligand binding. The acquisition of this unique property is intimately associated with the dynamics of the molecule.

Biological functions are, in general, regulated with the aid of proteins. Many proteins consist of more than one covalently linked structural domain, which individually exhibit distinct properties. Regulation of biological functions is generally realized by the interactions between these structural domains in the proteins. Thus, it is important to understand if these structural domains exert their functional properties independently or if unique properties are acquired when the domains are covalently linked. To address these issues, *Escherichia coli* cAMP receptor protein (CRP)[1] is employed as a model system.

CRP is a homodimer of 209 amino acid residues (*1*, *2*). As a global transcription factor, CRP regulates the expression of more than 150 genes in response to changes in intracellular cAMP levels (*3*−*6*). A modular protein in nature, CRP is a product of covalent linkage of two common structural domains. The N-terminal domain consists of the cyclic nucleotide binding site, which has served as a prototype for studying cyclic nucleotide selectivity and the molecular mechanism for activation by cyclic nucleotides in cyclic nucleotide-dependent protein kinases and cyclic nucleotide-gated channels (*7*−*11*). The C-terminal DNA-binding domain shows structure and sequence similarities to other gene regulatory proteins and is the founding member of this enlarging family of DNA-binding proteins (*12*−*18*). The helix−turn−helix motif formed by the E- and F-helices is highly conserved in many prokaryotic DNA-binding proteins (*18*, *19*). The binding of cAMP to the N-terminal domain of CRP allosterically enhances the binding affinity of the specific DNA in the C-terminal domain, and vice versa (*20*, *21*). cAMP binding exerts little effect on the secondary structure elements in either the N- or C-terminal domain of CRP, but it results in the exposure of F-helix to solvent to facilitate the binding to specific DNA (*22*−*25*). These observations are consistent with a proposed model that the cAMP-mediated structural changes in CRP involve rigid-body motions, including subunit realigment and domain reorientation, which lead to the activation of CRP (*26*, *27*). This model implies that these two domains communicate with each other by changing the tertiary structure and display functional properties when they are covalently linked. Thus, the functional and structural properties of native CRP represent the consequences of a covalent attachment of these two domains. To identify the unique properties acquired by this covalent linkage, an effective approach is to study these

† This work was supported by NIH Grant GM-45579 and Robert A. Welch Foundation Grants H-0013 and H-1238.

* To whom correspondence should be addressed. Phone: (409) 772-2281. Fax: (409) 772-4298. E-mail: jclee@utmb.edu.

‡ Current address: Department of Pharmacology and Toxicology, The University of Texas Medical Branch at Galveston, Galveston, TX 77555-1031.

[1] Abbreviations: CRP, cyclic AMP receptor protein; α-CRP, N-terminal domain of CRP; S-CRP and CH-CRP, α-CRP generated by subtilisin and chymotrypsin A digestion, respectively; β-CRP, C-terminal domain of CRP; IPTG, isopropylthiogalactopyranoside; Gu-HCl, guanidine hydrochloride; TEK (100) buffer, 50 mM Tri-base, 1 mM EDTA, and 100 mM KCl buffer at pH 7.8; Buffer A, 20 mM phosphate, 0.1 M KCl, 1 mM EDTA, 1 mM PMSF, 1 mM DTT, and 10% (v/v) glycerol at pH 7.5; Buffer B, 50 mM phosphate, 0.1 M KCl, 1 mM EDTA, 1 mM DTT, and 10% (v/v) glycerol at pH 7.5; Buffer C, 50 mM Tris, 0.02 M KCl, 1 mM EDTA, 1 mM DTT, and 10% (v/v) glycerol at pH 8.5; FT-IR, Fourier transform infrared spectroscopy; CPM, N^- [4-[7-(diethylamino)-4-methylcoumarin-3-yl] maleimide; FM, fluorescein 5-maleimide.

10.1021/bi026383q CCC: $22.00
Published on Web 11/15/2002

two domains separately and compare the properties of two separated domains with that of the intact CRP.

This study focuses on the isolated domains. The C-terminal domain, known as β-CRP, was cloned, expressed, and purified. The N-terminal domain, known as α-CRP, was obtained by proteolytic digestion of CRP. The structural properties of these domains were monitored by FT-IR, and the dynamics of these separated domains were compared with those in intact wild-type CRP.

EXPERIMENTAL PROCEDURES

Materials. Bacto-tryptone and yeast extract were from Difco. IPTG was purchased from Life Technologies. BL21-(DE3)/pLysS cells and pET8C vector were from the Molecular Biology Lab, UTMB. Chymotrypsin A was from Boehringer Mannheim. Subtilisin (protease type XXVII) and cAMP were purchased from Sigma. Ultrapure guanidine hydrochloride (GuHCl) was a product of ICN Biochemical. 99.96% Deuterium oxide (D_2O) was purchased from Cambridge Isotope Laboratories (Andover, MA).

Concentration Determination. The concentrations of proteins and cAMP were determined by absorption spectroscopy using the following absorption coefficients: 40 800 $M^{-1}cm^{-1}$ at 278 nm for CRP dimer (*20*); 3190 $M^{-1}cm^{-1}$ at 276 nm for β-CRP dimer (see Result); 14 650 $M^{-1}cm^{-1}$ at 259 nm for cAMP. Absorption spectra were measured using a Hitachi U-2000 spectrophotometer.

Cloning and Expression of β-CRP. β-CRP encoding amino acid residues 108−209 of CRP was generated by PCR using the following primers:

Upstream:
GCATGGATCCATGGTAAACCCGGACATTCTGATGCGT

Downstream:
GACTGGATCCAAGCTTAACGAGTGCCGTAAACGACGA

The product was cloned into the pET8C vector via restriction sites NcoI/BamHI and expressed in BL21(DE3)/pLysS cells. To maximize the expression of soluble β-CRP, an optimal condition of 100 μM of IPTG and 2.5 h of induction time was employed.

Purification of β-CRP. Ninety grams of BL21(DE3)/pLysS cells expressing β-CRP were suspended in 250 mL of Buffer A on ice. Cells were homogenized and lysed by a French Press at 10,000 psi. A soluble fraction was prepared by centrifugation at 15 000 rpm for 1 h. The supernatant was added and mixed gently with 30 g of Bio-Rax 70 gels equilibrated in Buffer A at 4 °C for 1 h. The mixture was packed into a column and washed with 200 mL of Buffer A. The column was eluted with a 0.1−1.2 M KCl linear gradient in a total volume of 200 mL of Buffer A at a flow rate of 0.9 mL/min. Fractions of 3.0 mL were collected and analyzed by SDS-PAGE. The fractions containing β-CRP were pooled. After adjusting the conductivity of the solution to the same as that of Buffer A by adding Buffer A without KCl, the solution was applied to a HTP gel (12 g of matrix) column preequilibrated with 120 mL of Buffer A. After washing with 120 mL of Buffer B, the column was eluted with a linear gradient of 0.1−1.2 M KCl in a total volume of 100 mL of Buffer B. Fractions containing β-CRP were pooled and dialyzed against Buffer C. The dialyzed solution was passed through a DEAE column (15 mL of gel matrix) equilibrated with 50 mL of Buffer C. The flow-through plus one column volume of washing was collected and dialyzed against Buffer A. Ammonium sulfate was added to the dialyzed sample to reach a final concentration of 1.0 M. The solution was applied to a 30 mL column of Phenyl Sepharose equilibrated with 1.0 M $(NH_4)_2SO_4$ solution in Buffer A. After washing with 100 mL of Buffer A with 0.8 M $(NH_4)_2SO_4$, the column was eluted with a linear gradient of 0.8−0 M $(NH_4)_2SO_4$ in a total volume of 160 mL of Buffer A. Fractions containing β-CRP of greater than 99% purity, as monitored by SDS−PAGE, were pooled and stored at −20 °C.

Amino Acid Sequence Analysis. Purified β-CRP was submitted to the Protein Chemistry Lab, supported by the UTMB Educational Cancer Center and the UTMB NIEHS Center, for sequencing analysis. N-terminal protein sequencing was done by using an Applied Biosystem, Inc. (ABI) 475A gas-phase protein/peptide microsequencer online with an ABI 120A PTH amino acid analyzer. Data were analyzed with an ABI 900A data analysis unit.

Preparation and Purification of α-CRP. S-CRP and CH-CRP were prepared and purified as described previously by proteolytic digestion of the purified wild-type CRP in the presence of cAMP using Subtilisin (protease type XXVII) and chymotrypsin A, respectively (*28*). Wild-type CRP was purified according to an established procedure (*20*).

Denaturation of β-CRP by GuHCl. GuHCl-induced denaturation of β-CRP was carried out in TEK (100) at 20 °C. Stock solutions of 7 M GuHCl in TEK (100) were prepared and filtered through a 0.45-μm filter. The final concentrations of the stock GuHCl solutions were determined by density measurement with a precision DMA-02D density meter (Mettler/Paar). Protein samples were equilibrated at 20 °C in varying concentrations of GuHCl for at least 1 h. The denaturation was monitored by circular dichroism.

Secondary Structure Determination by CD and FT-IR. Circular dichroism measurements were performed using an Aviv Model 60 DS spectropolarimeter. CD spectra were recorded over the range of 200−300 nm using a 1.0 cm pathlength cell. Protein concentration used in the FT-IR measurements was about 8 mg/mL. Two microliters of sample or buffer solution was injected into the cell of CaF_2 with 6μm path length and placed in the instrument holder for 10 min to reach temperature equilibrium. Then 200-scan, at the rate of 3 s/scan, single-beam spectra of protein solutions, buffer solutions, or vacant cell were collected with the resolution of 4 cm^{-1} at room temperature by using a BOMEM Fourier Transform Infrared Spectrometer (Quebec, Canada). The absorbance spectra of protein and buffer solutions were obtained by using "Absorbance" function in the software B_GRAMS/32 (BOMEM), where the single beam spectra of the empty cell were used as backgrounds. The absorbance spectra of protein were obtained by subtracting the absorbance spectra of buffer using the software PROTA (BOMEM). Secondary structure calculations were performed using the function "Factor Analysis" in the software PROTA. The secondary structural information of protein is reflected by the amide l band, which is located in the range of 1620−1700 cm^{-1}. This band is ascribed to >C═O stretching vibration of the peptide bond (*29*). The second derivative of the absorbance spectrum yields peaks in the region of 1682 to 1662, 1654, 1645, and 1632 cm^{-1}, corresponding to the structural elements of turns, α-helix, random coil, and β-sheet, respectively.

Sample Preparation by Lyophilization. A 100 μL sample of protein in TEK (100) was lyophilized for 2 h at room temperature. There was no significant difference in the contents of α-helices and β-sheets measured by FT-IR between the lyophilized and the unlyophilized protein (data not shown). Furthermore, there was no detectable difference in specific DNA-binding affinities. These results indicate that lyophilization of CRPs with buffer exerts no significant effects on their structures and functions. The reconstituted solutions were accurate representation of the solutions prior to lyophilization, as evidenced by the fact that the densities of these solutions, monitored by the high precision density meter, did not deviate more than 0.7%.

Protein Dynamics as Monitored by Hydrogen−Deuterium Exchange. Samples for exchange experiments were prepared by dissolving 100 μL of lyophilized CRP or buffer solution in 100 μL of D_2O. The reconstituted sample was injected into a CaF_2 window cell with a path length of 50 μm. One minute after the addition of D_2O, single-beam spectra were recorded using kinetic scanning mode at one minute interval. Twelve minutes after the addition, the interval for the kinetic scanning was changed to 5 min. The number of scans per time interval for these two kinetic scannings was 10 each at a rate of 3 s/scan. Subsequently, the number of scans was changed to 60 per time interval, and spectra were collected every 30 min. The amide ll band, located at about 1548 cm^{-1} that is ascribed to >N−H bending vibration in peptide bond, was employed to analyze protein dynamics. As >N−H in protein is exchanged into >N−D in D_2O, the absorption peak of >N−D bending vibration at about 1450 cm^{-1} is strengthened, while the >N−H absorption peak is decreased. Thus, the decrease in the >N−H absorption peak was used to monitor the dynamics of protein (*30*).

Sedimentation. Velocity sedimentation experiments were performed in a Beckman XL-A analytical ultracentrifuge with an An-60 Ti rotor, equipped with absorption optics. The experiments were carried out at 50 000 rpm and 20 °C using protein samples with absorbance at 280 nm ranging from 0.2 to 1.3 in TEK (100) buffer. Data were collected in the continuous mode. Results were analyzed using the DCDT+ program (Version 1.11) by John Philo.

The quaternary structure of β-CRP was monitored by sedimentation equilibrium. The experimental conditions were the same as in velocity experiments except that the speed was at 25 000 rpm. The data were fit by nonlinear least-squares analysis to obtain the reduced molecular weight according to

$$\sigma = M_r(1 - \bar{\nu}\rho)\omega^2/2RT \qquad (1)$$

where M_r is the molecular weight, $\bar{\nu}$ is the partial volume which assumes a value of 0.745 calculated from amino acid composition, ρ is the solvent density, ω is the angular velocity, and R and T are the gas constant and temperature in kelvin, respectively.

Mass Spectrometry. The matrix used in the experiments was 3,5-dimethoxy-4-hydroxycinnamic acid, at 10 mg/mL, in a solution containing 1:1:1 acetonitrile, ethanol, and 0.1% TFA (pH 2.5). The resulting matrix was adjusted to pH 2.5 with 2% TFA. Ten microliters of a 60μM solution of β-CRP was mixed with an equal volume of matrix solution, and 1 μL was spotted onto the MALDI target and air-dried at room temperature for about 10 min.

Matrix-assisted laser desorption ionization-time-of-flight (MALDI-TOF) mass spectra were acquired on a PerSeptive Biosystems Voyager DE STR. Data were obtained at a sampling rate of 2 GHz into 250 000 channels. Accelerating voltage was 20 kV, grid voltage 70%, and guide wire 0.01%. Delayed extraction was used with a nominal pulse delay of 100 ns. The manual laser intensity was typically 3000, and the signal with counts was typically 10 000. The data were acquired manually by accumulating traces at least six times for every sample. Cytochrome C, with a molecular weight of 12 361.5 Da was used as an external calibration standard.

DNA Binding. Fluorescence anisotropy measurements, using the SLM 8000C spectrofluorometer, were employed to monitor the binding of β-CRP to DNA. The detailed experimental, and data analysis protocols have been previously described (*31*). The DNA-binding sites were the 26 bp fragment of the *lac* P1 promoter with the sequence 5′-ATTAATGTGAGTTAGCTCACTCATTA-3′ and the random sequence 5′-CTCAGTTCTGATACCAAGCAGCCCAG-3′. The underlined sequence is the primary binding site for CRP. The reaction mixture contained 15 nM of DNA in TEK(100). Small volumes of concentrated β-CRP were titrated into the reaction mixture. The anisotropy of the CPM or FM-labeled DNA was measured after each addition of protein. The data were fitted to eq 2 by nonlinear least-squares (Sigmaplot) to determine the association constant for β-CRP-DNA interaction, K:

$$A = A_D + (A_{PD} - A_D) \times \frac{(KD_T + KP_T) + 1 - \sqrt{(KD_T + KP_T + 1)^2 - 4K^2D_TP_T}}{2KD_T}$$

where A is the measured value of anisotropy, A_D and A_{PD} are values of anisotropy associated with free DNA and β-CRP-DNA complex, respectively, and D_T and P_T are the total molar concentrations of DNA and dimeric protein, respectively.

RESULTS

Basic Characterization of β-CRP. Thirty-six cycles of automatic N-terminal protein sequencing of purified β-CRP revealed the following amino acid sequence: MVNPDILMRLSAQMARRLQVTSEKVGNLAFLDVTG. This sequence matched the sequence of 108−141 in wild-type CRP. The expected molecular weight for monomeric β-CRP is 11 284.3. With an additional terminal methionine residue, it becomes 11 415.5. The mass spectrum of purified β-CRP showed two peaks at 11 283.1±1.1 and 11 415.1±0.5, respectively, suggesting that the N-terminal methionine was partially cleaved in the expressed β-CRP.

Sedimentation velocity experiments showed that β-CRP sediments as a single symmetric boundary within a range of approximately 6-fold difference in protein concentration (Figure 1A). The goodness of fit of the profile to a single sedimenting species indicated that β-CRP exists as a homogeneous species with a value of 2.2 for $S_{20,w}$, as shown in Figure 1A. The molecular weight of β-CRP was monitored by sedimentation equilibrium and a typical result is shown in Figure 1B. The data fit well to a protein with a MW of 23 000±1,000. Combining the data from mass spectrometry and sedimentation, one may conclude that β-CRP is a dimer under the experimental conditions.

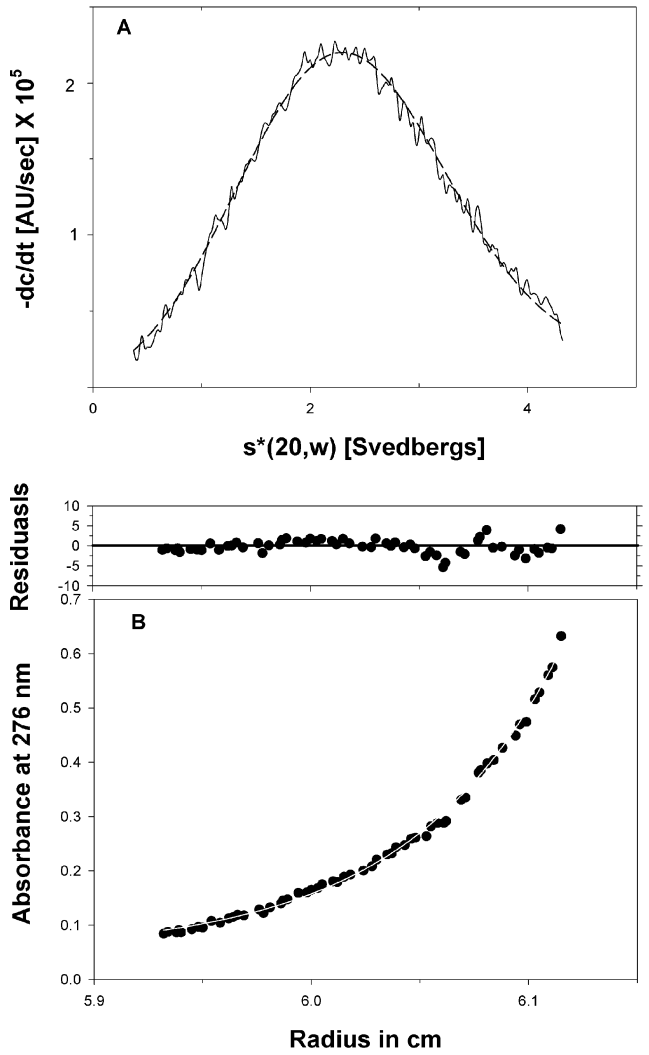

FIGURE 1: Sedimentation data of β-CRP. (A) Plots of -dc/dt vs apparent sedimentation coefficient corrected to water at 20 °C, s*-[20,w], for β-CRP in TEK (100). The data were fit to a one species model using the program DCDT+. The solid line was the experimental data, and the dashed line represented the best fit. (B) Sedimentation equilibrium data of β-CRP. The solid line was the fit. The residuals to the fit were shown in the upper panel.

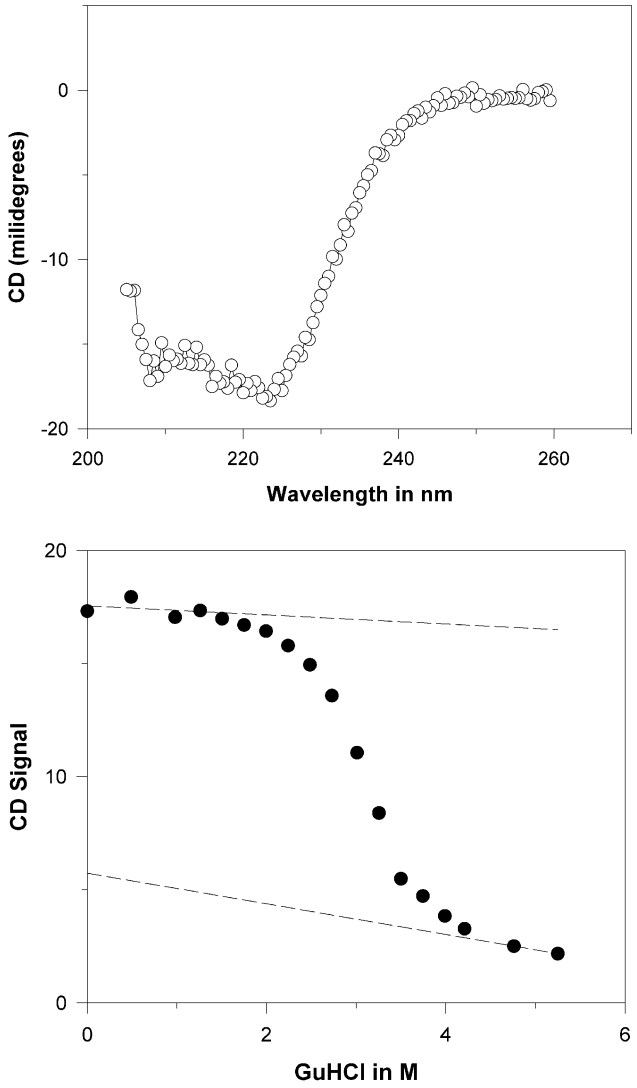

FIGURE 2: (A) Circular dichroism spectrum of native β-CRP. (B) Unfolding of β-CRP induced by GuHCl as monitored by CD at 222 nm. The concentration of β-CRP in panels A and B was 25μM in TEK(100).

The ultraviolet absorption spectrum of β-CRP showed a maximum absorption at 276 nm. When it was excited at 276 nm, a characteristic emission peak at 311 nm was observed. These spectral properties indicate that there is no tryptophan residue in β-CRP, as expected. The two tryptophan residues of CRP are in the N-terminal domain. On the basis of its amino acid sequence, the calculated molar absorption coefficient of monomeric β-CRP at 276 nm is 1595 $M^{-1}cm^{-1}$.

Secondary Structures of CRPs. The secondary structure of β-CRP was monitored by CD, as shown in Figure 2A. Maximal negative ellipticity was observed at 208 and 222 nm, indicating the presence of a significant amount of α-helix, a conclusion that is consistent with the crystallographic data that the C-terminal domain of CRP mainly consists of helices.

To test if β-CRP is a cooperatively folded structural entity, β-CRP was subjected to chemical denaturation by GuHCl. The results, as shown in Figure 2B, indicate that indeed the unfolding of β-CRP is cooperative in nature, suggesting that β-CRP is a folded domain.

The secondary structures of the various forms of CRP were investigated by FT-IR. The FT-IR absorbance spectra of β-CRP, S-CRP, CH-CRP, and wild-type CRP are shown in Figure 3A. The peaks that reflect the presence of α-helix and β-sheet were resolved in the second derivative spectra (Figure 3B). The content of α-helix was directly obtained from the calculations using the software PROTA (BOMEM) based on the FT-IR absorbance spectra. By using the second derivative spectra, the ratio of the peak areas for α-helix and β-sheet was obtained. The content of β-sheet was calculated from the ratio and the content of α-helix. The results are summarized in Table 1. Within experimental errors, these values are consistent with the calculated values based on the crystallographic data of wild-type CRP (*32*). These observations suggest that α-CRP and β-CRP assume the same distribution of secondary structures as that in the wild-type CRP.

Hydrogen−Deuterium Exchange. H/D exchange rates reflect on the internal motions of folded proteins. This technique is ideal for probing the structural flexibilities of the two linked or separated domains in CRP. The exchange reaction was complete within a couple of days, as indicated

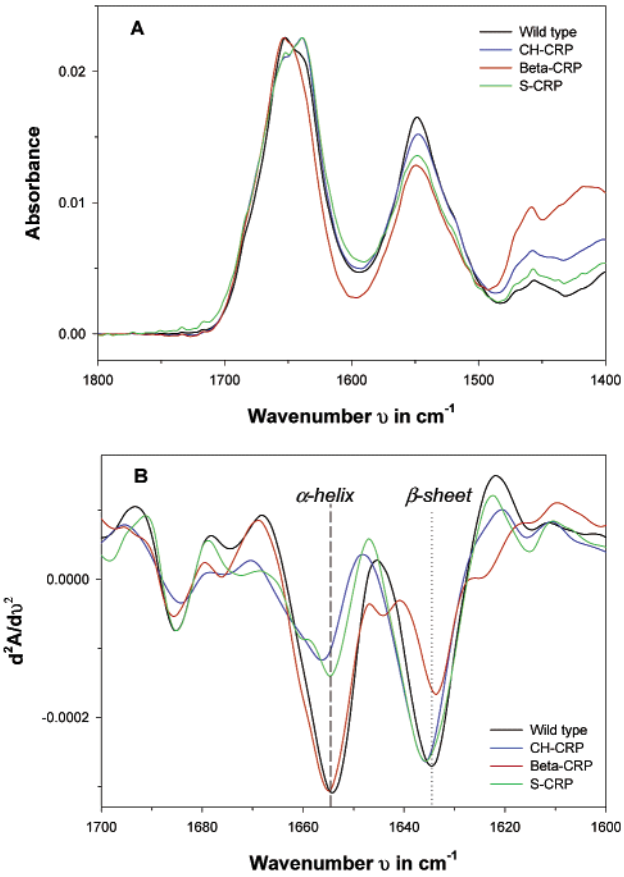

FIGURE 3: FT-IR spectra. (A) Absorbance spectra of wild-type CRP, CH-CRP, β-CRP, and S-CRP in TEK(100). The amide I band intensities of CH-CRP, β-CRP and S-CRP were normalized to that of wild-type CRP. (B) The second derivative spectra of amide I bands of panel A. The peaks at about 1654 and 1633 cm^{-1} are assigned to α-helices and β-sheets, respectively. The intensities of β-sheets of CH-CRP and S-CRP were normalized to that of β-sheets of wild-type CRP, while that of the α-helices of β-CRP was normalized to that of α-helices of wild-type CRP.

Table 1: The Content of α-Helices and β-Sheets in the CRPs

CRPs		wild-type CRP	S-CRP	CH-CRP	β-CRP
α-helices	exp.	35%	29%	31%	58%
	calc.[a]	38%	23%	32%	59%
β-sheets	exp.	35%	56%	48%	19%
	calc.[a]	38%	53%	45%	19%

[a] Calculated results in % based on the structure determined by X-ray crystallography (*32*).

by no further change in the spectrum spanning both the amide I and II bands. In CRP the absorbance intensity of amide I band (around 1650 cm^{-1}) increased only by about 7% for an exchange time of up to three weeks. Hence, the exchange reaction has little effect on the intensity of amide I band. On the contrary, the absorbance of amide II band (around 1550 cm^{-1}) was more sensitive to the exchange reaction (Figure 4A). The second derivative spectra, as shown in Figure 4B, indicate an obvious shift in peak from 1549.4 to 1543.7 cm^{-1} when the exchange time increased from 1 to 300 min in wild-type CRP. Furthermore, the area under the peak decreased with H → D exchange. Thus, the amount of nonexchanged amide protons was determined by integrating the area encompassed by the second derivative peak. To improve the accuracy and precision in determining the amount of exchange, the intensity of amide I band at 1 min

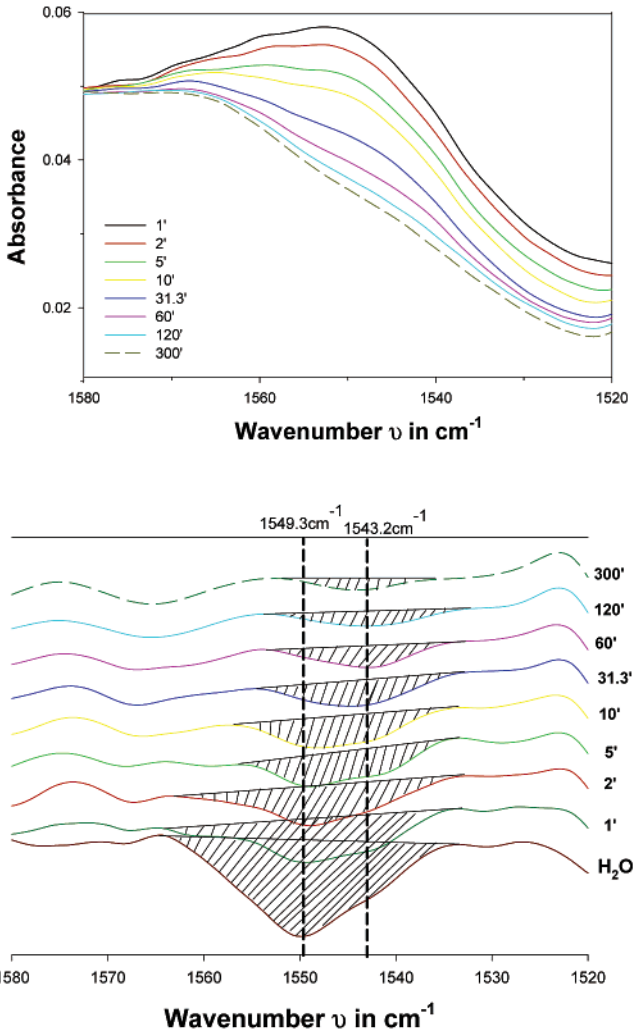

FIGURE 4: H/D exchange as monitored by FT-IR. (A) FT-IR absorbance spectra of >N−H bending vibration in wild-type CRP in 99.96% D_2O at different time. (B) The second derivative FTIR spectra of panel A. The shaded parts showed the integrated areas of >N−H at different time.

was used to normalize the area of amide II band at exchange time $t = 0$.

The fraction of nonexchanged amide proton, F, is expressed as

$$F = A_D/A_H \quad (3)$$

where A_D and A_H are the area encompassed by the second derivative peak of amide II band in D_2O and H_2O, respectively. In most cases, the fraction of nonexchanged amide protons at the first spectrum were less than 40%, as shown in Figure 5 and summarized in Table 2 in the column labeled F_o. Only CH-CRP was an exception. In this case, F_o is about 0.8. The data showed that approximately 80% of nonexchanged amide protons was present after one minute of exposure to 100% D_2O. A two-exponential model was used to describe the decay of the fraction of nonexchanged amide protons using eq 4

$$F = A_1 \exp(-k_1)t + A_2 \exp(-k_2)t + C \quad (4)$$

where A_i is the initial fraction of class i proton before exchange and k_i is the corresponding apparent exchange rate constant. In the present study, no physical significance is

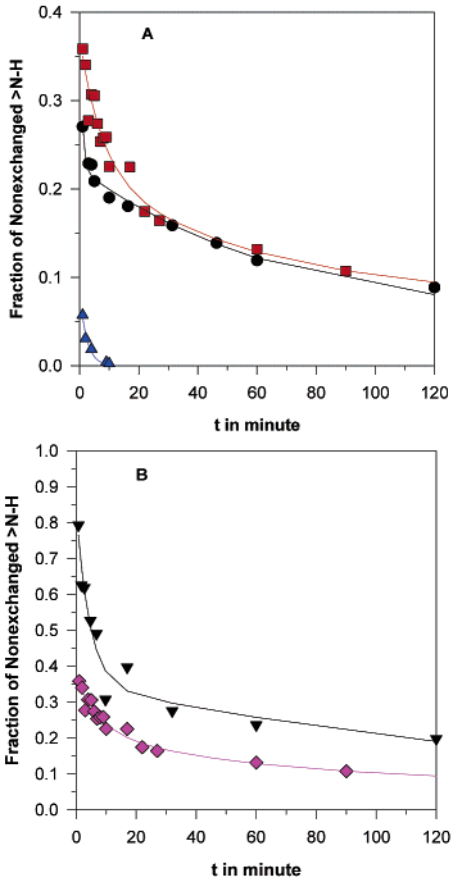

FIGURE 5: Normalized fractions of nonexchanged amide protons as a function of exposure time to D_2O measured with (A) wild-type CRP (●), S-CRP (■), and β-CRP (▲) and (B) CH-CRP (▼) and S-CRP (◆). The solid lines represent one or two-exponential fit to the data points.

attached to the resolved parameters except that these are grossly different classes of protons in accordance to their rates of exchange. The fitted data are listed in Table 2. β-CRP showed the fastest exchange. After 1 min of exposure to D_2O, less than 10% of the original amide protons were left.

Except β-CRP, the exchange kinetics of all the CRP species apparently can be resolved into at least three classes of amide protons with different exchange rates. There is a class that exchanges so rapidly that their exchange was completed before the first time point. In this study only two classes can be semiquantitatively monitored, as shown in Figure 5A,B. The apparent exchange rates differ by about 1 order of magnitude (Table 2). While wild-type CRP and S-CRP exhibit an approximately equal fraction of these two classes of amide protons, CH-CRP exhibits a larger fraction for both classes.

DNA Binding. The binding of β-CRP to DNA was monitored, as shown in Figure 6. The binding isotherms to *lac* and DNA of random sequence are superimposable. This

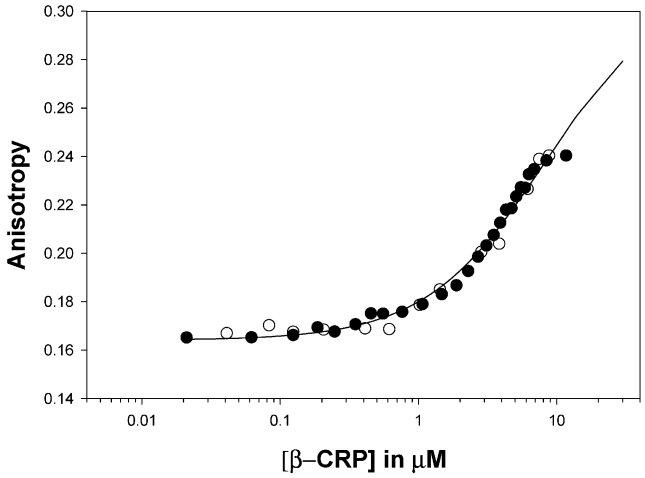

FIGURE 6: Binding isotherms of β-CRP to *lac* 26 (●) and random sequence (○) DNA in TEK(100) buffer at pH 7.8 and 25 °C. Concentration of DNA was 15 nM.

result indicates that β-CRP cannot distinguish between specific and nonspecific DNA sequences. The binding affinity was estimated to be $(1.2 \pm 0.2) \times 10^5$ M^{-1}, which is close to that of intact wild-type CRP to *lac* in the absence of cAMP.

DISCUSSION

Upon binding of cAMP to the N-terminal domain of wild type CRP, the affinity of the C-terminal domain for specific DNA is significantly enhanced. On the basis of the principle of thermodynamic reciprocity, binding of DNA should enhance the affinity of CRP for cAMP. This basic principle is observed in the ternary complex formation involving CRP. For example, the binding affinity of cAMP to D53H CRP is changed from 4.1×10^4 to 3.5×10^7 M^{-1} in the presence of lac26 DNA, and the DNA binding affinity to lac26 is increased from 2.4×10^6 to 2.1×10^9 M^{-1} by the addition of cAMP.[2] These results indicate that the cAMP- and DNA-binding domains communicate with each other in CRP. The issue is the mechanism of communication. The mechanism of allosteric communication upon cAMP binding has been proposed to involve intersubunit interaction through the C-helices, principally T127 and S128, mediated by the C^6 amino group of cAMP, and rearrangement of the stereo-orientation between the two domains via the hairpin loop between β4 and β5 (*32*). The residues T127 and S128 are crucial for the allosteric activation of CRP (*22*, *26*, *33*). However, the loop between β4 and β5 is thought to be likely important for the transmission of ligand signals (*34*, *35*). Much of the specificity in DNA recognition resides in the DNA-binding domain (*36*). These molecular events are the results of the intricate network of communication in CRP, which is a product of covalent linkage of two popular protein structural modules. It is of interest to define the independent

Table 2: Fitted Exchange Parameters[a]

CRP	F_o	A_1	A_2	k_1 (min^{-1})	k_2 (min^{-1})	c
wild type	0.27 ± 0.02	0.11 ± 0.02	0.15 ± 0.02	0.3 ± 0.1	0.012 ± 0.003	0.05 ± 0.01
S-CRP	0.36 ± 0.02	0.15 ± 0.05	0.15 ± 0.05	0.14 ± 0.07	0.017 ± 0.009	0.08 ± 2.02
CH-CRP	0.79 ± 0.04	0.50 ± 0.07	0.35 ± 0.05	0.23 ± 0.07	0.005 ± 0.002	0
β-CRP[b]	0.06 ± 0.02	0.08 ± 0.01	–	0.42 ± 0.07	–	0

[a] F_o is the nonexchanged fraction at one-minute after exposure. [b] The exchange of β-CRP is fitted to equation for one exponential.

properties of the two domains and to gain insights into the unique properties acquired by a covalent linkage of the two domains.

α-CRP (S-CRP and CH-CRP) and *β*-CRP represent the N- and C-terminal domain of wild-type CRP, respectively. In either α-CRP or *β*-CRP, no significant change in the secondary structures was detected by comparing the substructures of the same part in wild type CRP (Table 1). The verification of the predicted distributions of secondary structures in wild-type CRP and its separate domains by FT-IR data means that the formation of secondary structures in the two domains are likely to be independent in wild-type CRP, although there are most likely minor structural changes that are not detected by FT-IR. The covalent linkage of these domains does not impart observable gross alteration in secondary structures. The communication between these two domains due to cAMP or specific DNA binding must originate from the tertiary/quaternary structural changes in the binding domains and possibly subunit-subunit realignment. This interpretation is consistent with the observation that in the CRP-cAMP complex, the domains within the two subunits have different orientations (*26*). In the "open" subunit, there is a large cleft between the domains, while the cleft is not present in the other "closed" subunit. When bound to DNA, both subunits are in the "closed" conformation (*37*, *38*). The structural changes resulted from the ligand bindings are delivered to the other domain. In a thermodynamic term, the energy of binding is propagated to the other domain by the connections between these two domains and results in a redistribution of the conformational ensemble (*39*, *40*).

The lack of observable changes in secondary structures as a consequence of covalent linkage implies that the effects on domain properties have to be probed by techniques that are sensitive to subtle changes of structural conformation and dynamics. Hence, the dynamics of CRP and the separate domains are investigated by H/D exchange. All amide protons (>N−H) in proteins can be roughly divided into three classes (*41*, *42*). Class 1, fast exchange protons, is most likely located on the surface or in regions that are totally accessible to solvent. Class 2, the amide protons with intermediate rates, is located in flexible buried regions or secondary structural elements that are not part of the core region. Class 3, slow exchange fraction, is predominantly located in the core region of the protein. Hydrogen−deuterium exchange of the amide protons is a measurement of the flexibility/dynamics of a protein. In general, conformational flexibility/dynamics is important to the function of a protein. After 1 min of exchange, the data showed that a significant amount of amide protons in CH-CRP and S-CRP are not exchanged as indicated by the larger values of F_o = 0.79 and 0.36, respectively, while *β*-CRP showed the least with a value of 0.06 for F_o. These data indicate that the C-terminal domain is much more dynamic than the N-terminal domain. After one-minute of exposure to D_2O, the fraction of nonexchanged >N−H in wild-type CRP is 0.27. The observation that F_0 is less than that of α-CRP is a surprising result. One might expect the reverse order if one considers the surface area exposed to solvent. In CRP, intuitively one might expect to have less solvent exposed surface area than the summation of the two separated domains due to the domain-domain interaction induced by covalent linkage.

Let us examine the effect of the C-helix. Although the crystallographic data show that the C-helix constitutes extensively the subunit-subunit interface, both S-CRP and CH-CRP are dimers with similar association constants (*28*). In Class 1 amide protons of α-CRP, the H/D exchange rate of S-CRP is much faster than that of CH-CRP (Figure 5). The difference between CH-CRP and S-CRP is that in CH-CRP the whole C-helix is preserved, whereas in S-CRP 85% of the C-helix is deleted. It means that the C-helix exerts a significant effect on either the exposure of the N-terminal domain to solvent or the dynamic motion of the domain. The difference in the number of residues between CH- and S-CRP is only about 20, i.e., less that 20% of the total number of residues in S-CRP. Yet, the presence of these residues in the form of C-helix in CH-CRP leads to a significant increase in F_0 to 80%, a 2-fold increase in comparison to S-CRP. Thus, the increase in 20 residues cannot account for this large increase in slow exchange protons in CH-CRP. This increase in F_0 implies that the C-helix reduces the dynamic behavior of the N-terminal, cAMP binding domain.

Although the whole C-helix is retained in CH-CRP, there is no large difference between the Stokes radii of CH-CRP and S-CRP (*28*). For the larger CH-CRP to assume the same Stokes radius as the smaller S-CRP, CH-CRP has to be more compact. The more compact structure of CH-CRP may obstruct the contact with solvent molecules. However, an equally probable mechanism can be proposed to rationalize the experimental result; i.e., the C-helix is not a dynamic entity, and its slow exchange rate might account for the differences in the exchange behavior between CH- and S-CRP. At present, there is no information to distinguish these possible mechanisms. The effect of the C-helix on the DNA-binding domain can only be inferred. *β*-CRP without the C-helices is very unstable and cannot be expressed to any significant amount (*43*). The poor expression could be the consequence of instability of the domain and is highly susceptible to proteolytic degradation. The exchangeable protons in such an unstable entity can be expected to exchange very rapidly. The fact that a small fraction of nonexchanged proton can be detected in *β*-CRP implies that the C-helices might induce slower dynamic motions in the *β*-CRP domain as it does in α-CRP.

The value of ∼0.3 for F_0 in full length CRP is approximately of the same magnitude as the sum of that of S-CRP and *β*-CRP, 0.42. This calculation is made possible because the area encompassed by the absorbance band is proportional to the amount of amide protons and the fraction of nonexchanged proton of the two domains can be expressed as $(F_S + F_\beta) \approx (A_{SD} + A_{\beta D})/A_{SH}$. A_{SH} and $A_{\beta H}$ are the areas of the nonexchanged >N−H absorption peaks of S-CRP and *β*-CRP in H_2O, respectively; A_{SD} and $A_{\beta D}$ are their areas in D_2O, respectively, and F_S, and F_β are their nonexchanged >N−H fractions, as summarized in the second column of Table 2. As there are approximately the same number of residues in S-CRP and *β*-CRP, one might set $A_{SH} \approx A_{\beta H}$. The similarity of the calculated result and the observed value (0.4 vs 0.3) for $(F_s + F_\beta)$ is different from the estimated value for $(F_{CH} + F_\beta)$, ∼0.85. Remembering that the difference between CH- and S-CRP is the presence in the C-helix in CH-CRP, the result of this comparison implies

[2] Lin, S.-H. and Lee, J. C. *Biochemistry* (in press).

that the presence of the C-terminal, DNA-binding domain in wild-type CRP can overcome the stabilizing effect of the C-helix. The validity of such a conclusion is being further investigated.

CH-CRP and S-CRP lack the DNA-binding domain; however, in an earlier study, it was shown that they could bind cAMP with approximately the same binding affinity in comparison with wild-type CRP (*28*). This indicates that the ability to bind cAMP is maintained in this domain and the C-helices do not play a significant role in ligand recognition. Nevertheless, the C-helices affect the communication between the ligand binding sites (*28*). The two sites in S-CRP show no cooperativity, while those in CH-CRP show significant negative cooperativity (*28*). In a recent study, as a result of extensive investigation of cAMP binding to wild type and mutant CRPs, it was shown that wild-type CRP exhibits two sets of cAMP binding sites, two sites per set. The pair of high-affinity sites exhibits positive cooperativity (*44*). These results are consistent with the binding study reported by Gorshkova et al. (*45*) and the structural study of Won et al. (*46*). The opposite degree of cooperativity observed in CH-CRP and wild-type CRP implies that the presence of the rest of β-CRP can modulate the effect of C-helices. It is most interesting to note the report by Tanaka and co-workers on a chimeric protein that consists of the cyclic nucleotide binding domain from bovine retinal rod ion channel and the DNA-binding domain from CRP (*36*). Although the specificity for ligand in the channel is cGMP > cAMP, the chimeric protein shows reverse efficiency in activation. These results imply that the DNA-binding domain assists in conferring ligand specificity. Thus, CRP exists as a network of communication, and the proper arrangement of all the structural components within the protein are crucial for functional signal transmission.

Concluding Remark. The covalent linkage between two independent domains can lead to unique properties that are essential for intermolecular communications. These properties are not necessarily associated with significant structural changes. Perturbations in structural dynamics are the consequences in covalent linkage in CRP. Intramolecule signal transmissions between the two covalently linked domains, triggered by ligand binding, are required for the completion of CRP activation (*25*, *44*). Thus, it is useful to exercise caution in ascribing structure−function correlations of multidomain proteins. One should not simply consider the summation of properties of individual domains.

REFERENCES

1. Aiba, H., Fujimoto, S., and Ozaki, N. (1982) *Nucl. Acids Res. 10*, 1345−1361.
2. Cossart, P., and Gicquel-Sanzey, B. (1982) *Nucl. Acids Res. 10*, 1363−1378.
3. Adhya, S., and Garges, S. (1990) *J. Biol. Chem. 265*, 10797−10800.
4. Busby, S., and Buc, H. (1987) *Microb. Sci. 4*, 371−375.
5. de Crombrugghe, B., Busby, S., and Buc, H. (1984) *Science 224*, 831−838.
6. Reznikoff, W. S. (1992) *J. Bacteriol. 174*, 655−658.
7. Taylor, S. S., Buechler, J. A., and Yonemoto, W. (1990) *Annu. Rev. Biochem. 59*, 971−1005.
8. Shabb, J. B., and Corbin, J. D. (1992) *J. Biol. Chem. 267*, 5723−5726.
9. Goulding, E. H., Tibbs, G. R., and Seilgelbaum, S. A. (1994) *Nature 372*, 369−374.
10. Shabb, J. B., and Corbin, J. D. (1992) *J. Biol. Chem. 267*, 5723−5726.
11. Zagotta, W. N., and Siegelbaum, S. A. (1996) *Annu. Rev. Neurosci. 19*, 235−263.
12. Brennan, R. G. (1993) *Cell 74*, 773−776.
13. Clark, K. L., Halay, E. D., Lai, E. and Burley, S. K. (1993) *Nature 364*, 412−420.
14. Liang, H., Olejniczak, E. T., Mao, X., Nettesheim, D. G., Yu, L., Thompson, C. B., and Fesik, S. W. (1994) *Proc. Natl. Acad. Sci. U.S.A. 91*, 11655−11659.
15. Ramakrishnan, V., Finch, J. T., Graziano, V., Lee, P. L., and Sweet, R. M. (1993) *Nature 362*, 219−223.
16. Schwartz, T., Rould, M. A., Lowenhaupt, K., Herbert, A., and Rich, A. (1999) *Science 284*, 1841−1845.
17. Spiro, S., and Guest, J. R. (1990) *FEMS Microbiol. Rev. 6*, 399−428.
18. Steitz, T. A., Ohlendorf, D. H., Mckay, D. B., Anderson, W. F., and Matthews, B. W. (1982) *Proc. Natl. Acad. Sci. U.S.A. 79*, 3097−3100.
19. Harrison, S. C., and Aggarwal, A. K. (1990) *Annu. Rev. Biochem. 59*, 933−969.
20. Heyduk, T., and Lee, J. C. (1989) *Biochemistry 28*, 6814−6924.
21. Takahashi, M., Blazy, B., Baudras, A., and Hillen, W. (1989) *J. Mol. Biol. 207*, 783−796.
22. Won, H.-S., Yamazaki, T., Lee, T.-W., Yoon, M.-K., Park, S.-H., Otomo, T., Kyogoku, V., and Lee, B.-J. (2000) *Biochemistry 39*, 13953−13962.
23. Baichoo, N., and Heyduk, T. (1997) *Biochemistry 36*, 10830−10836.
24. Baichoo, N., and Heyduk, T. (1999) *Protein Sci. 8*, 518−528.
25. Dong, A., Malecki, J. M., Lee, L., Carpenter, J. F., and Lee, J. C. (2002) *Biochemistry 41*, 6660−6667.
26. Harman, J. G. (2001) *Biochim. Biophys. Acta 1547*, 1−17.
27. Cheng, X., and Lee, J. C. (1998) *Biochemistry 37*, 51−60.
28. Heyduk, E., Heyduk, T., and Lee, J. C. (1992) *Biochemistry 31*, 3682−3688.
29. Susi, H., and Byler, D. M. (1986) *Methods Enzymol. 130*, 290−311.
30. Susi, H., and Byler, D. M. (1983) *Biochem. Biophys. Res. Commun. 115*, 391−397.
31. Heyduk, T., and Lee, J. C. (1990) *Proc. Natl. Acad. Sci. U.S.A. 87*, 1744−1748.
32. Passner, J. M., Schultz, S. C., and Steitz, T. A. (2000) *J. Mol. Biol. 304*, 847−859.
33. Cheng, X., Kovac, L., and Lee, J. C. (1995) *Biochemistry 34*, 10816−10826.
34. Scott, S.-P., and Tanaka, J. C. (1998) *Biochemistry 37*, 17239−17252.
35. Scott, S.-P., and Tanaka, J. C. (1995) *Biochemistry 34*, 2338−2347.
36. Scott, S.-P., Weber, I. T., Harrison, R. W., Carey, J., and Tanaka, J. C. (2001) *Biochemistry 40*, 7464−7473.
37. Passner, J. M., and Steitz, T. A. (1997) *Proc. Natl. Acad. Sci. U.S.A. 94*, 2843−2847.
38. Schultz, S. C., Shields, G. C., and Steitz, T. A. (1991) *Science 253*, 1001−1007.
39. Pan, H., Lee, J. C., and Hilser, V. J. (2000) *Proc. Natl. Acad. Sci. U.S.A. 97*, 12020−12025.
40. Lin, S.-H., Kovac, L., Chin, A. J., Chin, C. Q., and Lee, J. C. (2002) *Biochemistry 41*, 2946−2955.
41. Kim, K. S., Fuchs, J. A., and Woodward, C. K. (1993) *Biochemistry 32*, 9600−9613.
42. de Jongh, H. H., Goormaghtigh, E. and Ruysschaert, J. M. (1995) *Biochemistry 34*, 172−179.
43. Gronenborn, A. M., and Clore, G. M. (1986) *Biochem. J. 236*, 643−649.
44. Lin, S.-H., and Lee, J. C. (2002) *Biochemistry 41*, 11857−11867.
45. Gorshkova, I. T., Moore, J. L., McKenny, K. H., and Schwarz, F. P. (1995) *J. Biol. Chem. 270*, 21679−21683.
46. Won, H.-S., Lee, T. W., Park, S.-H., and Lee, B. J. (2002) *J. Biol. Chem. 277*, 11450−11455.

BI026383Q